ISSN: 2788-7669

Metamaterial Inspired Frequency Reconfigurable Antenna for Sub 6GHz Applications

¹Sakthevel T C and ²Sugumar D

1,2 Department of Electronics and Communication Engineering, Karunya Institute of Technology and Sciences, Coimbatore, Tamil Nadu, India.
¹saktheveltc20@karunya.edu.in, ²sugumar@ieee.org

Correspondence should be addressed to Sakthevel T C: saktheveltc20@karunya.edu.in

Article Info

Journal of Machine and Computing (https://anapub.co.ke/journals/jmc/jmc.html)

Doi: https://doi.org/10.53759/7669/jmc202606001

Received 10 June 2025; Revised from 02 August 2025; Accepted 19 September 2025

Available online 13 October 2025.

©2026 The Authors. Published by AnaPub Publications.

This is an open access article under the CC BY-NC-ND license. (https://creativecommons.org/licenses/by-nc-nd/4.0/)

Abstract – The antenna's design and frequency reconfiguration have a significant impact on its performance, which makes it perfect for a particular use case such as the Internet of Things. In this, study developed a unique metamaterial patch antenna design using a frequency reconfiguration technique. In the study, the metamaterial microstrip patch antenna (MMPA) was deployed in an Internet of Things application utilizing a frequency reconfiguration approach, achieved with the help of a PIN Diode. Changing the bias of two PIN diode switches altered the resonating frequency. An FR-4 substrate with a copper patch forms the proposed antenna. The suggested antenna construction has dimensions of 23 x 19 mm^2 . Two steps are involved in the design of a reconfigurable multiband antenna. The first designed Monopole for a Single Band with a centre frequency of 4.0GHz and the Second designed Multiband using a Rectangular Split Ring Resonator (RSRR) on the Ground Plane which includes two PIN diodes as switches, is evaluated in the ON-ON, OFF-ON, ON-OFF, and OFF-OFF switching scenarios. Antenna performance parameters like Gain, reflection coefficient, radiation efficiency, and standing wave ratio of voltage are used to estimate the presentation of the suggested antenna. At the Operating frequency of 3.6 GHz, the suggested antenna's efficiency and gain are 1.68 dB and 81%, respectively.

Keywords – Metamaterial Microstrip Patch Antenna (MMPA), Frequency Reconfigurable, Rectangular Split Ring Resonator (RSRR), Internet of Things (IoT).

I. INTRODUCTION

The billions of physical objects that make up the global network known as the Internet of Things (IoT) exchange data without the need for human input. IoT is being used in many different areas, such as automation, smart homes, buildings, manufacturing, healthcare facilities and transportation. It makes data analysis and decision-making possible in real-time.[1]. CISCO Systems predicts that by 2024, roughly 30 billion gadgets will use IoT technology, outnumbering people by more than fourfold [2]. For IoT applications, the RA (Reconfigurable Antenna) has more options for designing to obtain resonance frequency. The Metamaterial helps to reduce antenna size and improve reconfigurability. The SRR (Split Ring Resonator) is formed by two or more metallic rings, taken as twisted in a pattern that is circular, rectangular, or square. An antenna's structure can produce a metamaterial with unique permeability and permittivity properties by including SRR. As a result, metamaterials are often referred to as artificial materials. Certain antenna properties, like as gain, bandwidth, and directivity are improved as a result of metamaterials. In holographic applications, metamaterial improves radiation pattern control and sidelobe cancellation.

The tuning of sensitive wireless setup devices frequently requires the use of a tuned resistance or varactor diode. Because of its potential applications in communications, electronic monitoring and countermeasures, Reconfigurable Antennas have attracted a lot of interest lately. Switching in RAs allows the radiating element's form to change. Reconfiguration of frequencies has garnered significant attention in recent times, mostly due to the starter of novel ideas in WC (Wireless Communication). Many switching technologies are reconfigurable, such as optical switches, PIN diodes, Field Effect Transistors (FET), and Radiofrequency MEMS switches [3]. However, a thorough demonstration of PIN-diode integration with the antenna has not been completed. This study presents a unique frequency-RA design with a Square Split Ring Resonator (SSRR) for the IoT application. Initially, we designed the monopole microstrip patch antenna with a centre frequency of 4 GHz. The proposed metamaterial construction of a Rectangular Split Ring Resonator (RSRR) comprises switching PIN diodes to facilitate frequency reconfiguration and RSRR structure was used to make a tiny antenna.

The remainder of the paper is organized as follows: Section 2 presents the literature review; Section 3 presents the proposed methodology. Section 4 provides an overview of the results. Section 5 contains the work's conclusion.

II. RELATED WORK

The author developed a small WIPT (wireless information and power transmission) system integrated with metamaterial [4]. The less power regime powers the many IoT sensors. The proposed antenna operated at dual-band (900 MHz and 405 MHz). Two defective ground structure-based resonators, in which two single band resonating structures are cascaded to create WIPT.

Using FR-4 substrate material, the author created a mixed-floral square-shaped split ring resonator antenna. The antenna uses a frequency range of 7.6 GHz to 7.94 GHz to service the satellite application [5].

The decagon antenna designed by author [6] which operates at frequency range of 2.40-2.50 GHz. The complementary split ring resonator with metamaterial structure used to make the decagon antenna for wireless application.

The Ultra-Wide Band antenna designed for application in WiFi, Bluetooth and Zigbee technology [7]. The microstrip feeder with complementary split ring resonator utilized in the design of antenna.

The CRLH-TL MTM was constructed using the Rogers RT5880 substrate, which has a relative permittivity of 2.2 and a thickness of 0.787 mm. The composite right-left-hand transmission line metamaterial structure is based on an interdigital capacitor unit cell and is constructed using a meandering line [8].

A tiny electrical antenna operating at 0.9 GHz was constructed by the author [9] for use in radio frequency identification applications. The antenna was 30 mm by 30 mm by 1.6 mm. The antenna is designed and verified using the HFSS tool.

The suggested design in [10] comprises of a Microstrip Patch antenna. An SRR and a semicircular-shaped SRR on the ground plane make up the patch antenna. The dimensions of the substrate (FR4) used to create this ESA are 20 mm x 18 mm \times 1.6 mm. The HFSS tool was used to simulate the recommended antenna. The ESA can attain a 300 MHz bandwidth (700 MHz–1000 MHz) at 0.9 GHz, according to the simulated data. This is the recommended antenna for the global mobile communication system.

RF energy harvesters are a possible long-term solution for driving IoT devices and wireless networks, as proposed in [11]. This first setting, as far as I can tell, makes use of a frequency-self-adaptive radio frequency harvester that makes use of shape-reconfigurable liquid metal to efficiently detect and convert any random signal that falls between 1.8 and 2.6 GHz

This work [12] uses a frequency reconfigurable antenna with CFSRR (Complementary Four SRR) for wireless communication applications. The Rogers RT5880 dielectric has dimensions of L=38 mm \times w=21 mm \times h=1.6 mm, a ε_r = 2.2, and a dissipation factor of 0.0009. This surface has the recommended antenna written on it. The proposed antenna has a VSWR of less than 1.5 in all resonant bands, indicating its efficacy and reliability.

For 5G portable devices application, the reconfigurable MIMO antenna with an Electromagnetic Band Gap structure with four radiating components is developed in [13]. Planar Monopole Radiating Elements with Coplanar Waveguide Ports (CWPs) are used in the array. It is shown that by inductively connecting the radiating element to the Minkowski fractal structure of the first order, better impedance matching improves the bandwidth performance of the array. The EBG structure in a MIMO array provides the isolation between antenna components.

In [14], The proposed patch antenna makes use of half-moon-holed ellipse and rectangular strip lines to operate in dual bands. RF-MEMS switches were proposed along the rectangular strip lines of the patch antenna to provide reconfigurability. The suggested elliptical antenna is designed to operate with a capacitive shunt-type RF switch. The proposed RF-MEMS switch can tolerate beam stress up to 85.7 MPa, has a displacement of 3µm, and an actuation voltage of 5.02 V. The reconfigurable elliptical patch antenna has a reflection coefficient of -32.28 dB at 8.34 GHz and -22.7 dB at 10.47 GHz, respectively.

In [15], the author describes an antenna with frequency retuning and pattern diversity driven by metamaterials. In MIMO applications, pattern diversity is achieved by combining two reconfigurable structures on a single antenna to create two distinct orthogonal patterns. Surface-mounted varactors that can switch the operating frequencies of both radiation patterns from 1.7 to 2.2 GHz can cover the 1.71-2.17 GHz LTE spectrum.

A novel wearable antenna had a metamaterial structure inspired monopole apple shaped with UC-EBG (Unipolar compact Electromagnetic Bandgap) that operates at triple band for biomedical applications [16]. By including metamaterial TCSRR (Triangular CSRR) into the antenna and UC-EBG construction, a small UC-EBG-backed antenna measuring 39 mm × 39 mm × 2.84 mm is produced. The frequencies for 5G new radio (NR) include 3.5 GHz, 2.45 GHz for wireless local area networks (WLANs), and 5.8 GHz for ISM bands. At these early frequencies, the printed textile antenna has better gain and higher efficiency.

A radiation-reconfigurable antenna in the n78 band is presented in [17] for 5G applications. A U-shaped strip and a tuning fork work together to produce a radiating element from a planar monopole. There is a section of ground maintained at the back. Radiation reconfigurability is achieved in this design by using four metamaterial unit cells—two on each side of the radiator. Comb-shaped metamaterial unit cells, arrayed clockwise and linked to the radiator by BAR-64-02V PIN diodes, encircle the antenna.

The study focuses on novel linear and dual-polarized antennas for 5G and 6G networks, medical devices, Internet of Things technologies, and health monitoring [18]. Passive and active sensors can operate independently by collecting electromagnetic radiation and charging the wearable sensor's battery by mounting an energy-harvesting device on the antenna.

In this paper, [19] proposes a very small microstrip antenna array for MIMO operating at 6 GHz frequency ranges. The array consists of two components. The antenna is made up of an IDC and a meander line that is conjugate when activated by a monopole basic antenna.

Table 1. Performance Comparison of Literature Antenna

	Table 1. Performance Comparison of Literature Antenna					
Ref. No	Author	Reconfigurable Process	Material Used	Methods Of Meta Material Designed	Size Of Reconfigurable Antenna	Resonance Band
[12]	Amal Mohamme d Rasool et al.	Frequency re- configurable antenna	Four Split Ring Resonators (SRR)-based metamaterial	Two PIN diodes	(38×21×1.6) mm ³	In operating frequency at 1.8, 2.3, 3.0, 4.1, 5, and 6.4 GHz < 10 dB (reflection coefficient).
[14]	ketavath kumarnaik et al.	A compact dual- band reconfigurable elliptical-shaped patch antenna	FR 4	RF-MEMS switches	28x30x1.6	8.34GHz and 10.47GHz
[15]	Jiahao Zhang et al.	An antenna that is varactor-tuned and inspired by metamaterials, with frequency reconfigurability and pattern diversity	Rogers R04003	varactor- tuned	150 mm x 150 mm	1.7 GHZ to 2.17 GHZ (LTE band)
[22]	Sherif A. Khaleel et al.	For higher data rate and wider bandwidth proposed reconfigurable system	Two Port MIMO- MPA antenna	utilizing G RIS	120X90 (μm²)	functions with a resonance frequency of 1.9 THz.
[23]	Hayder H. Al- Khaylani et al.	Novel linear and dual-polarized antennas for 5G and 6G networks, medical equipment, Internet of Things technologies, and health monitoring are the main topics of this study.	FR4 substrate	two photo resistors and two varactor diodes	istors and o varactor $62 \times 40 \times 1.6$	operating between 3.6 and 4.9 GHz, which are the three resonant frequencies
[26]	Sunil P. Lavadiya et al.	Frequency reconfigurable	split-ring resonator	Roger RT duraid	66.4 mm ²	3 GHz–9 GHz
[27]	Bashar Ali Esmail et al.	Reconfigurable CSR MM structure.	Printed dipole antenna	On the dielectric layer of the antenna, a 2 × 3 array of reconfigurab le MM	12 mm X16 mm	large bandwidth in the 28 GHz frequency.

The suggested antenna in [20] is made up of an inner spiral resonator that is loaded into an outer SRR. It may be modified remotely using SPDT switches or PIN diodes. The tiny antenna, which is $22x16x \ 1.6 \ \text{mm}$ 3, may function in triband or broadband mode depending on whether the switches are in the ON or OFF position. Either two CG2415M6 SPDT switches or two BAR6402V PIN diodes functioning as RF switches are used to accomplish frequency reconfigurability. Arduino units are used to remotely operate SPDT switches.

Subwavelength operation and phase manipulation are two properties of metamaterials that have several applications in 5G communication systems. High data speeds, processing power, efficiency, affordability, small size, and low power consumption are requirements for both current and future 5G equipment. An overview of metamaterials and their effects on performance improvement and use in communication systems (5G and 6G) is given in [21].

An AMC (Artificial Magnetic Conductor) made of graphene can be used to growth the gain of the antenna. The G AMC layer of the MIMO antenna sits below the G-RIS layer and increases the gain from 4.5 dB to 10 dB in [22]. For MIMO applications, the recommended antenna design between G-RIS and G-AMC is useful.

A printed MPA with MTM additions is recommended in this study [23] for contemporary sub-6 GHz spectrum applications such as 5G. The antenna consists of a T-stub resonator connected to a printed microstrip line with discontinuities. The proposed microstrip line is connected with two spiral-top circuits and four fractal MTM unit cells. The antenna is driven by photoresistors with two varactor diodes and a coplanar waveguide.

For 5G mobile networks, a printed monopole antenna with cascading multi-stage metamaterial (MTM) unit cells is created [24]. A printed copper trace and four T-Resonators (TR) structures to accommodate four MTM unit cells make up the recommended antenna. This combination, when combined with a coplanar waveguide (CPW) feed, increases the antenna's gain and bandwidth at sub-6GHz bands. Taconic RF-43 substrate is used to construct the antenna. As a result, the recommended antenna takes approximately 51 x 24 mm2 of effective space.

Using PIN diode switches, the author describes in [25] an MTM superstrate-based MPA appropriate for wireless network applications. Microstrip antennas employ metamaterials as the superstrate, such as square and circular arrays. The superstrate layers strengthen the antenna's overall structure and enhance its properties, such as gain and bandwidth, to function as a radome.

The frequency reconfigurable antenna [26] design for application of weather forecast, satellite communication and raw satellite feed. The size of the antenna summary by the split ring resonator achieved by the PIN diode with patch.

This study [27] used two distinct refractive indices and a millimeter-wave (MMW) band to develop a reconfigurable metamaterial (MM) structure. The principal beam of the antenna is directed in a 5G band at 28 GHz using these two MM designs.

A 25×25 mm2 (LSub×WSub) antenna that may be adjusted for five frequency bands is shown in this work [28]. Through the use of slot designs, corner truncation, and parasitic loading, the antenna has optimum frequency responses. A synchronized module of three P-I-N diodes' high-frequency switching characteristics is composed of individual responses.

The various reconfigurable antenna design approaches, meta material design methodologies, antenna size and resonance frequency are described based on the following **Table 1**.

Section 3 presents the geometric features of the metamaterial-based frequency reconfigurable antenna and the monopole microstrip patch antenna. Additionally covered are the switching mechanism and antenna design process. The results of the metamaterial-based frequency reconfigurable antenna performance comparison are validated in Section 4. In Section 5, the paper is finally ended.

III. THE GEOMETRIC DETAILS OF THE MONOPOLE ANTENNA AND PROPOSED FREQUENCY RECONFIGURABLE ANTENNA

Monopole Microstrip Patch Antenna

The Monopole Antenna was calculated and designed for 3.5GHZ and corresponding Dimensions Optimization was done with CST Studio Suite Simulation software to make the Centre Frequency as 4GHZ. **Fig 1** illustrates the monopole microstrip design. The complete sizes of the antenna are "23 mm x 19 mm" (Length x Width). The monopole antenna design is fabricated using 1.6 mm thick FR4 substrate. A substrate with a Tangent loss of $\delta = 0.025$ and a dielectric constant of $\varepsilon_r = 4.3$. A microstrip line has a 50 Ω impedance connection. The ground plane is printed on one side of the substrate, while the patch and microstrip line are printed on the other side. The width and length of the microstrip feed is denoted by the symbols WF and LF. The width and length of patch is denoted by WP and LP.

Maintain the same lengths for the partial ground plane and microstrip line to ensure good impedance matching. The precise numbers for every part of the antenna are displayed in **Fig 1**.

The microstrip patch antenna's dimensions were estimated using transmission line theory. The patch's width may be approximated as follows:

$$W = \frac{c}{2*Fc*\sqrt{\varepsilon_{reff}}} \tag{1}$$

The length of the patch is calculated from the below formula

$$L = \frac{c}{4*Fc*\sqrt{\varepsilon_{reff}}} \tag{2}$$

Here, ε_{reff} -Effective relative permittivity (substrate FR-4) Effective Relative Permittivity of the FR4 substrate c- Speed of light

Fc-Operating frequency

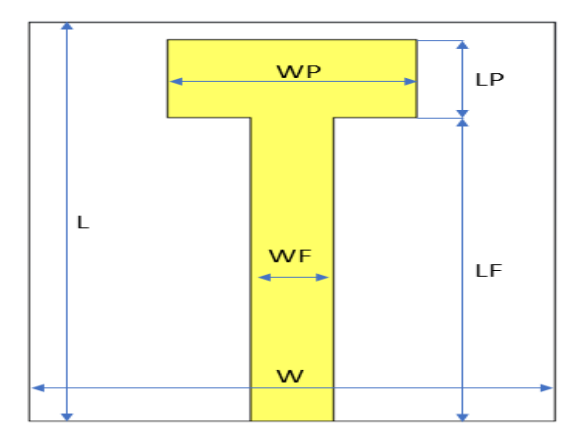


Fig 1. Geometrical Configuration of Monopole Antenna.

The Proposed Metamaterial-Based Frequency Reconfigurable Antenna

Using microstrip patch antenna approaches, the geometry of a rectangular patch is modified to generate the MMPA (Metamaterial Microstrip Patch Antenna). A rectangular split ring resonator (RSRR) located on the ground plane makes up the innovative antenna design. To minimize the total antenna size, split ring resonators are used. **Table 2** contains design metrics, while **Fig 2** details several perspectives of the suggested antenna configuration. The antenna length and form of the radiating element may be changed by utilizing two PIN diodes to accomplish reconfigurability.

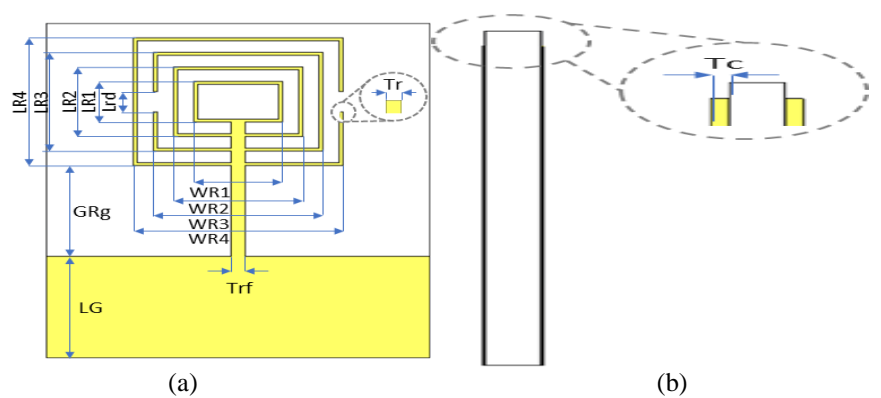


Fig 2. MMP Antenna Different View (A) Rear View (B) Side View.

Fig 2a depicts the rectangular split ring resonator (RSRR), which consists of four rings and two diode gaps for PIN diode placement. The suggested antenna's performance is numerically analyzed using CST Studio Suite Simulation software, a commercial electromagnetic simulation software program. The proposed MMPA consists of 4 rectangular split-ring resonators. The Width and Length of the Rectangular Split-Ring is denoted by the symbol LR1, WR1 and LR2, WR2 and LR3, ER3 and LR4, WR4. The Ground plane length is denoted as LG. The Gap between the ground plane and outer ring is denoted as GRg. The Thickness of the ring is denoted as Tr. The Gap of the ring to place the Pin diode is denoted as Lrd.

Table 2. Proposed MMPA 's Dimension Parameter

Antenna Parameters	Size of parameter (mm)	Antenna Parameters	Size of parameter (mm)
L	23	Lrd	3
W	19	LR1	2.8
LP	0.035	LR2	4.8
LF	17.5	LR3	6.8
WP	9	LR4	8.8
WF	3	WR1	4.4
LG	7	WR2	6.4
GRg	6.2	WR3	8.4
RG	1	WR4	10.4
Tr	0.2	Tc	0.035

Fig 3. displays the suggested constructed antenna model. rectangular split ring resonator (RSRR) without a diode is shown in Fig 3a and RSRR with a PIN diode is presented in the 3b.

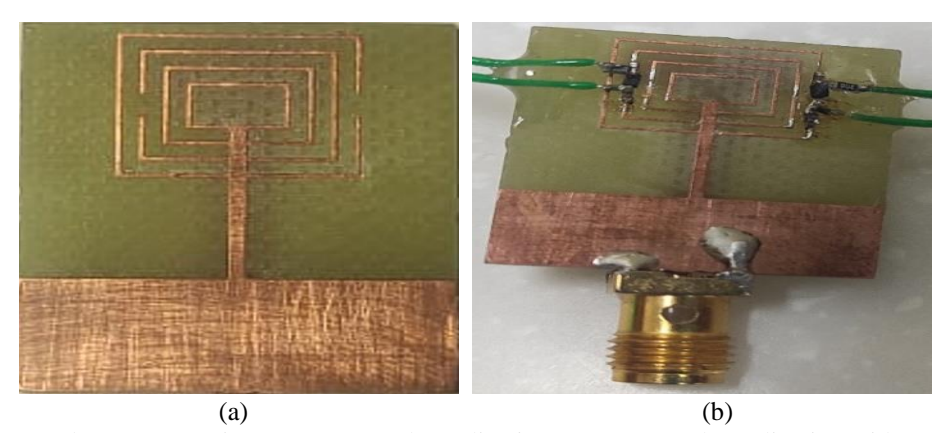


Fig 3. The Proposed Antenna Design (A) Rectangular Split Ring (B) Rectangular Split Ring with Two PIN Diodes.

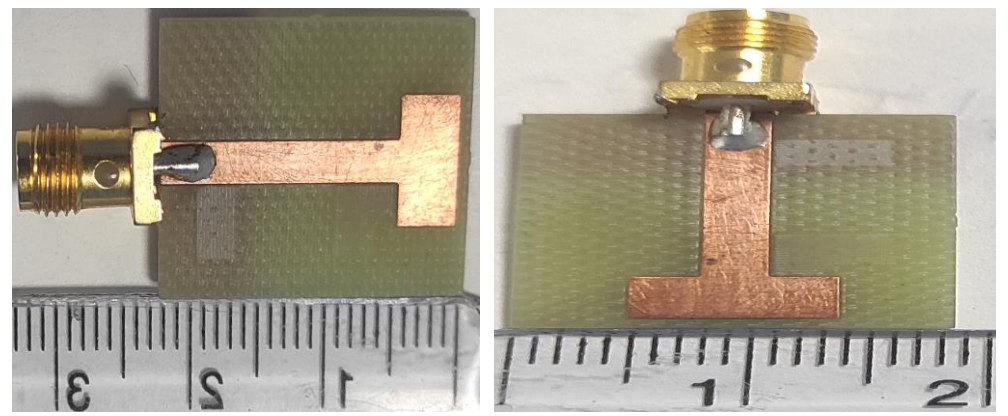


Fig 4. Fabricated Monopole Antenna with Geometric.



Fig 5. The Reflection Coefficient was Verified with the KEYSIGHT Fieldfox Microwave Analyzer N9917A.

Frequency tunability is an important requirement in reconfigurable antenna. In this work, two PIN diodes are used to achieve the frequency reconfigurable due to a change in charge distribution on the ground side. **Fig 5** represents the fabricated proposed antenna with KEYSIGHT FieldFox Microwave Analyzer N9917A. As per the Design consideration, when both the PIN Diodes are Forward Biased observed that the required current was drawn from the power supply. This confirms the function of the PIN diode with its suitable Bias circuit as expected in the RF path. The frequency at operates RSRR is calculated from the base formula (3).

$$fo = \frac{1}{2*\pi*\sqrt{L*C}} \tag{3}$$

$$fo = \frac{1}{2*\pi*\sqrt{Lm*(Cm+Cgap)}}\tag{4}$$

$$Ctot = Cm + Cgap (5)$$

$$fo = \frac{1}{2*\pi*\sqrt{Lm*Ctot}}\tag{6}$$

Lm-Represents Inductance of each Metallic Ring

$$Lm = \frac{\mu o * Rg}{Tr} * [LR4 + LR3] \tag{7}$$

Cm-Represents Space between the Inner and Outer Ring

$$Cm = \frac{A*\varepsilon o*\varepsilon r*Tr*(2*LR4+2*LR3-Lrd)}{2*Rq}$$
(8)

Cgap-Represents Space between the Ring Cut

$$Cgap = \frac{\varepsilon o * \varepsilon r * tc}{Lrd} \tag{9}$$

Fig 6 and 7 depict the PIN diode model in the CST microwave studio and the pin diode's electric equivalent circuit respectively. The configuration that is being described illustrates how frequency may be reconfigured by adjusting the PIN diode's on/off switch position.

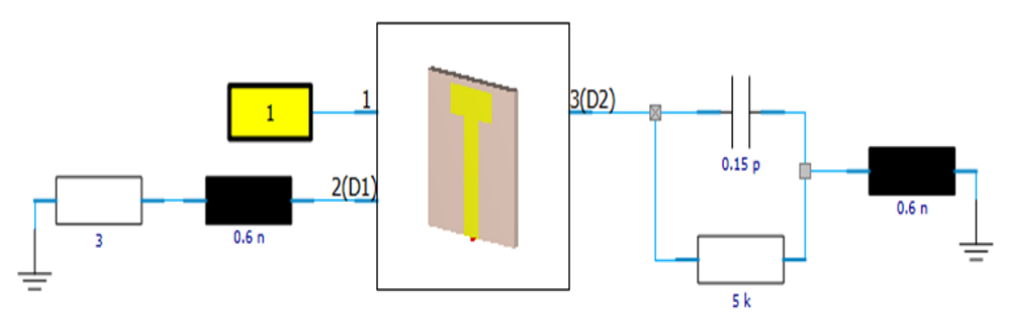


Fig 6. PIN Diode Model in Simulation Tool.

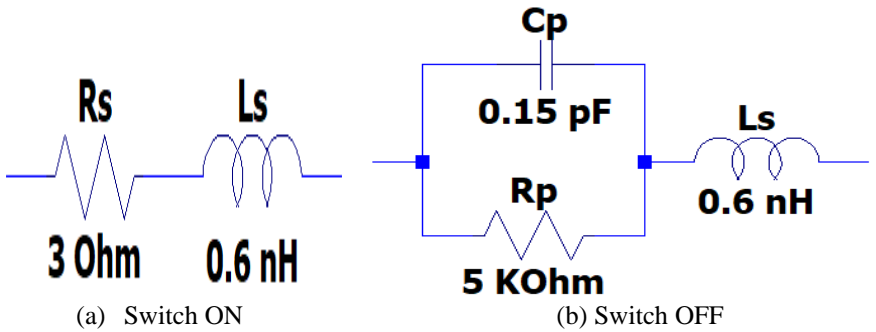


Fig 7. Represents the (a) ON (b) OFF State of the PIN Diode.

A resistor (R_s) and an inductor (L_s) linked in series indicate the switch-on condition in **Fig 7**. For the switch-off state, the resistor (R_p) and capacitor (C_p) are connected in series with the inductor (L_s) . **Table 3** displays the PIN diode's forswitching mode.

Table 3. Four Switching Modes of PIN Diode

= ····· = · · · · · · · · · · · · · · ·					
Switch mode		PIN diode (D1)	PIN diode (D2)		
	SM1	OFF	OFF		
	SM2	ON	OFF		
	SM3	OFF	ON		
	SM4	ON	ON		

From **Table 3**, the SM1 represents the two PIN diodes in the OFF condition. SM2 represents the D1 in the ON condition and D2 in the OFF condition. For SM3, D1 is OFF and D2 is ON. In SM4, all the diodes are in ON condition. The P-I-N diode technical specification is shown in **Table 4**.

Table 4. Technical Specification of PIN Diode

Part Number	BAR50-02V-H6327
Package	PG-SC79-2-1
Frequency Range	10 MHz up to 6 GHz
DIODE 'ON' Parameter	Ls=0.6nH & Rs=3 Ohm
DIODE 'OFF' Parameter	Cp=0.15pF & Rp=5 Kohm

IV. RESULT AND DISCUSSION

The fabricated monopole antenna with geometric is exposed in **Fig 4**. The Monopole Antenna was calculated and considered for 3.5GHZ and corresponding Dimensions Optimization was done with CST Simulation tool to make the Centre Frequency as 4GHZ. **Fig 8** depicts *the* S_{11} parameter of the monopole antenna.

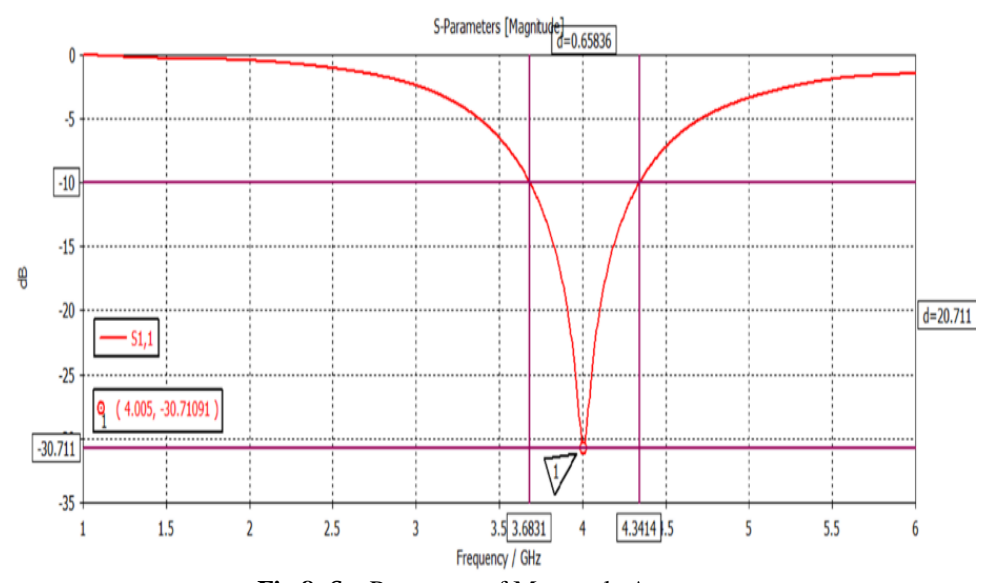


Fig 8. S_{11} Parameter of Monopole Antenna.

Fig 9 displays the S_{11} plot of monopole antenna at frequency range of 1.8 GHz to 5.4 GHz. Two metrics are used to assess the veracity of simulated outcomes using an artificial design structure. The first one is reflectance response (S_{11}). Multiple Frequency was achieved by implementing the Rectangular Split Ring and Design Optimization was done. From **Fig 9**, S1,1(37) found the best Optimized Result, shown in **Fig 10** Multiple Frequency achieved with Two PIN Diode Switching (D1 & D2).

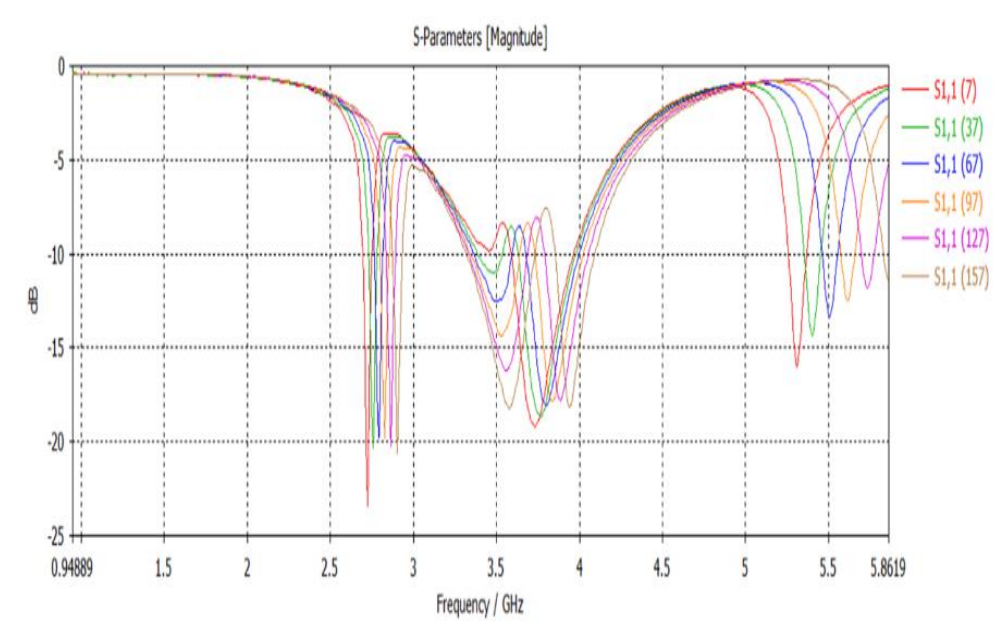


Fig 9. S_{11} Parameter of MMPA with RSRR Structure.

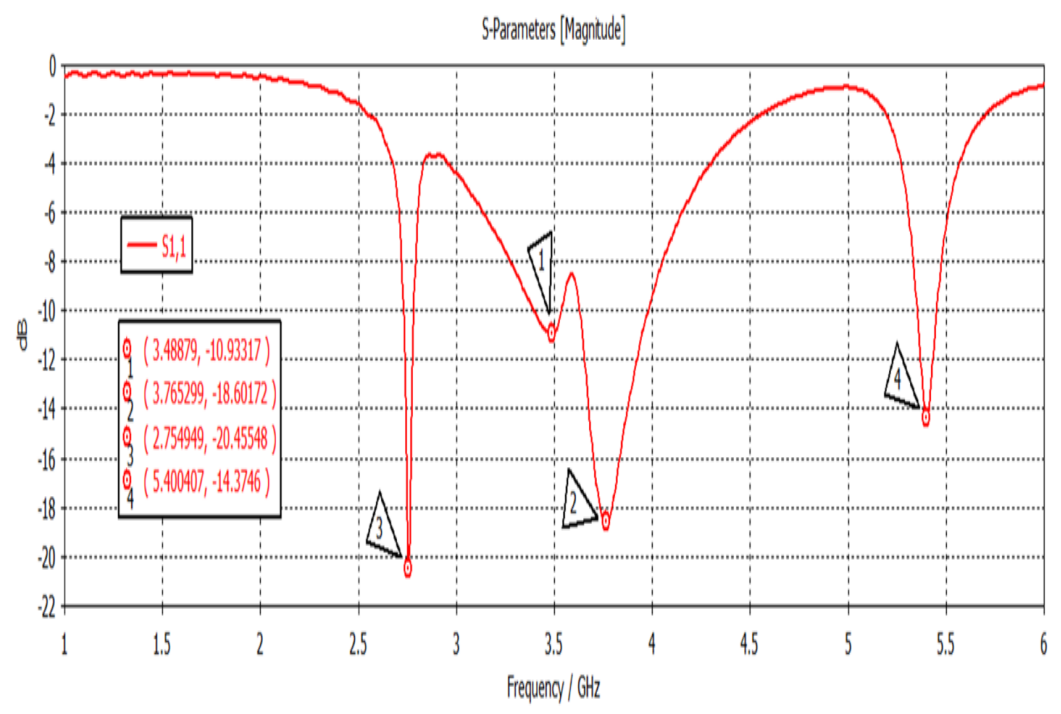


Fig 10. Multiple Frequencies with Optimized S_{11} Parameter.

Phase and amplitude measurements of the incident and reflected signals are used to calculate the S_{11} parameter, which is reached when the output of the test system approaches its ideal characteristic impedance (z_0).

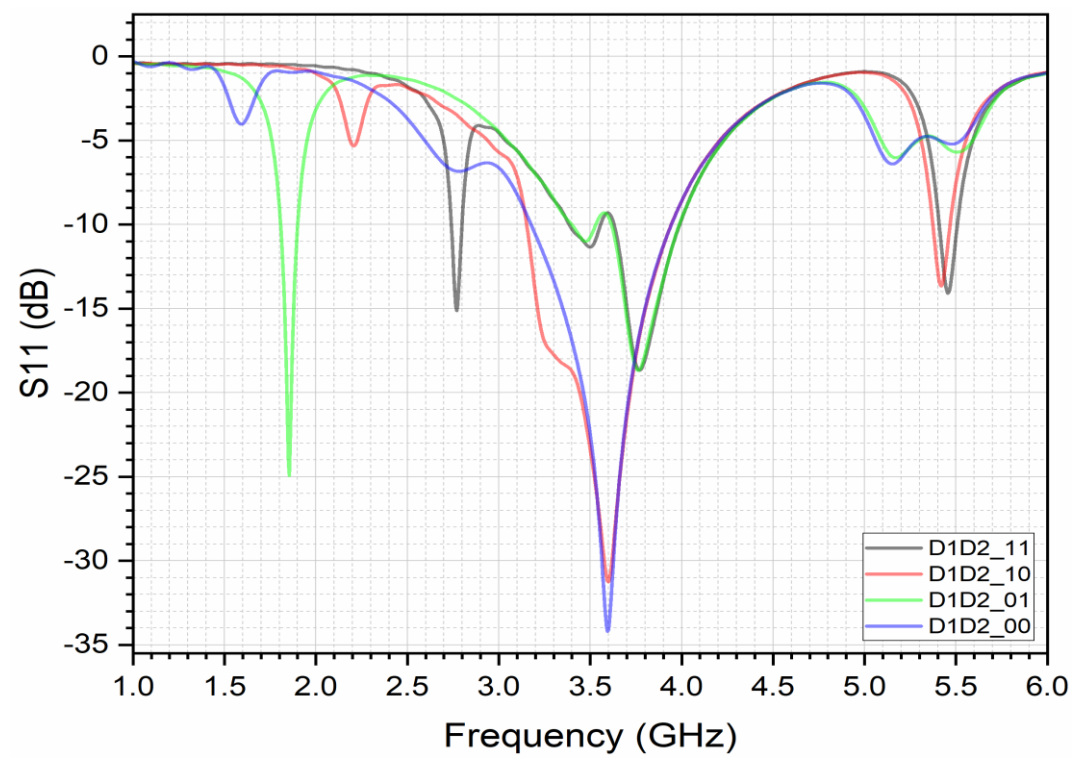


Fig 11. S_{11} Parameter of Proposed MMPA with RSRR.

Fig 11 illustrates S_{11} parameter of the different switching mode of the proposed antenna. the signal strength range, power efficiency, and system performance are calculated from the radiation efficiency metrics. The outcome shows that the suggested antenna is a good fit for sub-6GHZ applications due to its small size. the VSWR parameter of the proposed MMPA with RSRR are shown in **Fig 12**.

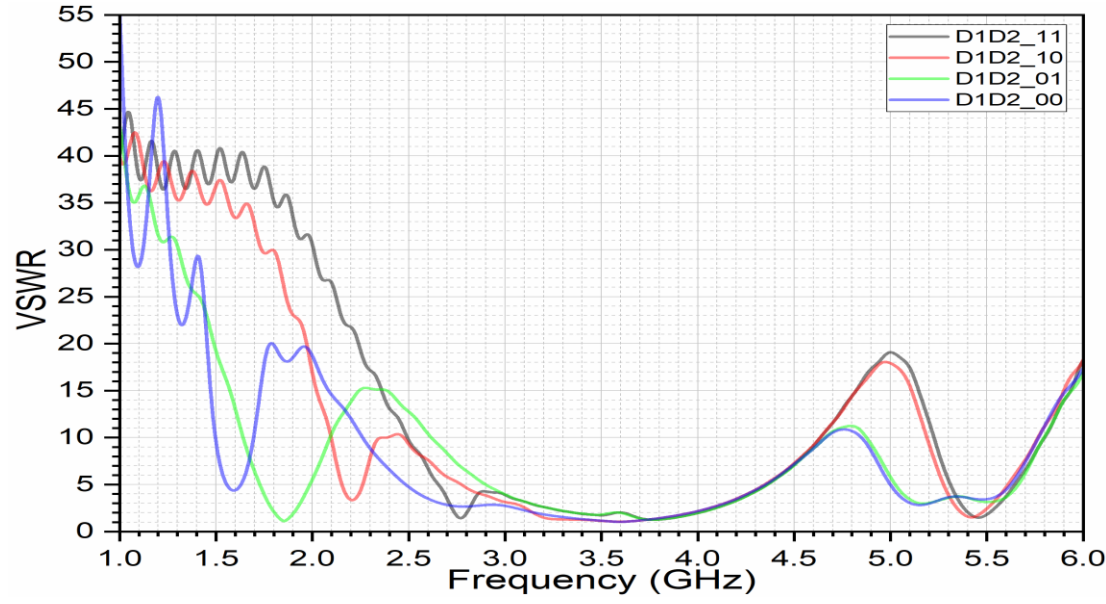


Fig 12. VSWR of Proposed MMPA with Different Frequencies Achieved by Configuration of PIN Diode.

Fig 13 displays the radiation pattern of simulated antennas at various mode of operation. It is shown that the MMPA generates a bidirectional pattern in the E plane and H planes and has good performance. Fig 13(a), 13(b), 13(c), and 13(d) depicts the radiation pattern of the various switching modes (SM1, SM2, SM3, and SM4).

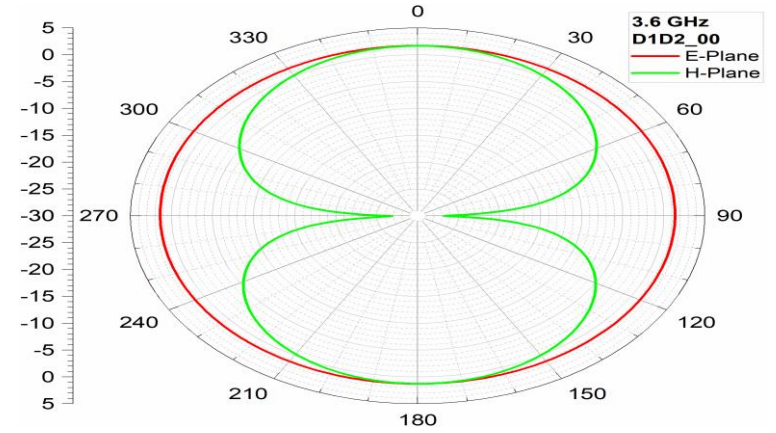
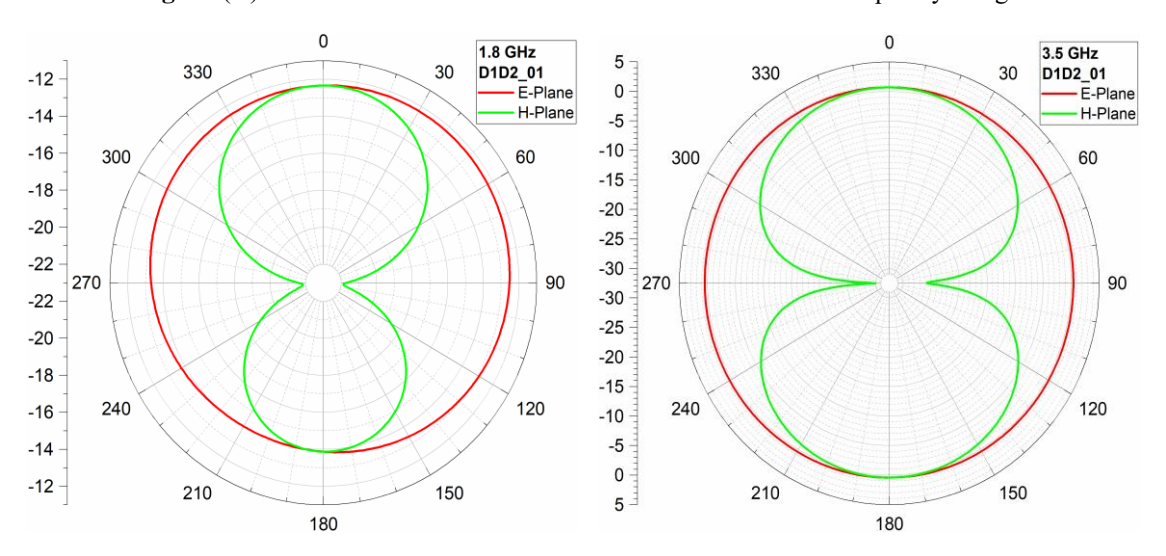


Fig 13. (A) MMPA's Radiation Pattern at SM1 State at 3.6 GHz Frequency Range.



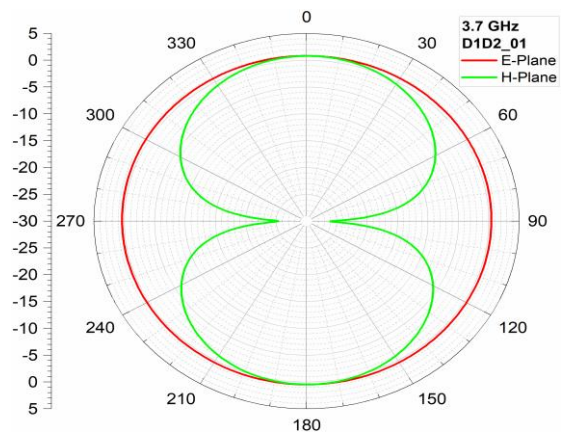


Fig 13. (B) Radiation Pattern of MMPA at SM2, Operates at Three Different Frequency Ranges 1.8ghz, 3.5 GHz, and 3.7 GHz.

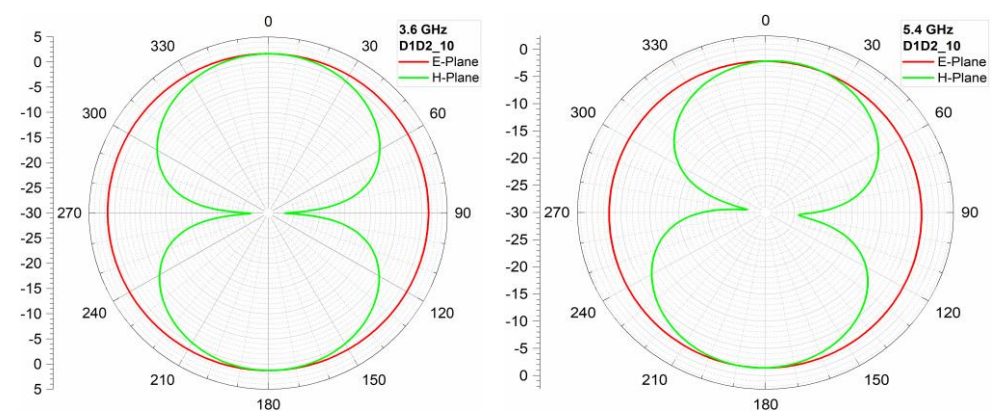


Fig 13. (C) Radiation Pattern of MMPA at SM3, Operates Two Frequency Ranges 3.6 GHz and 5.4 GHz.

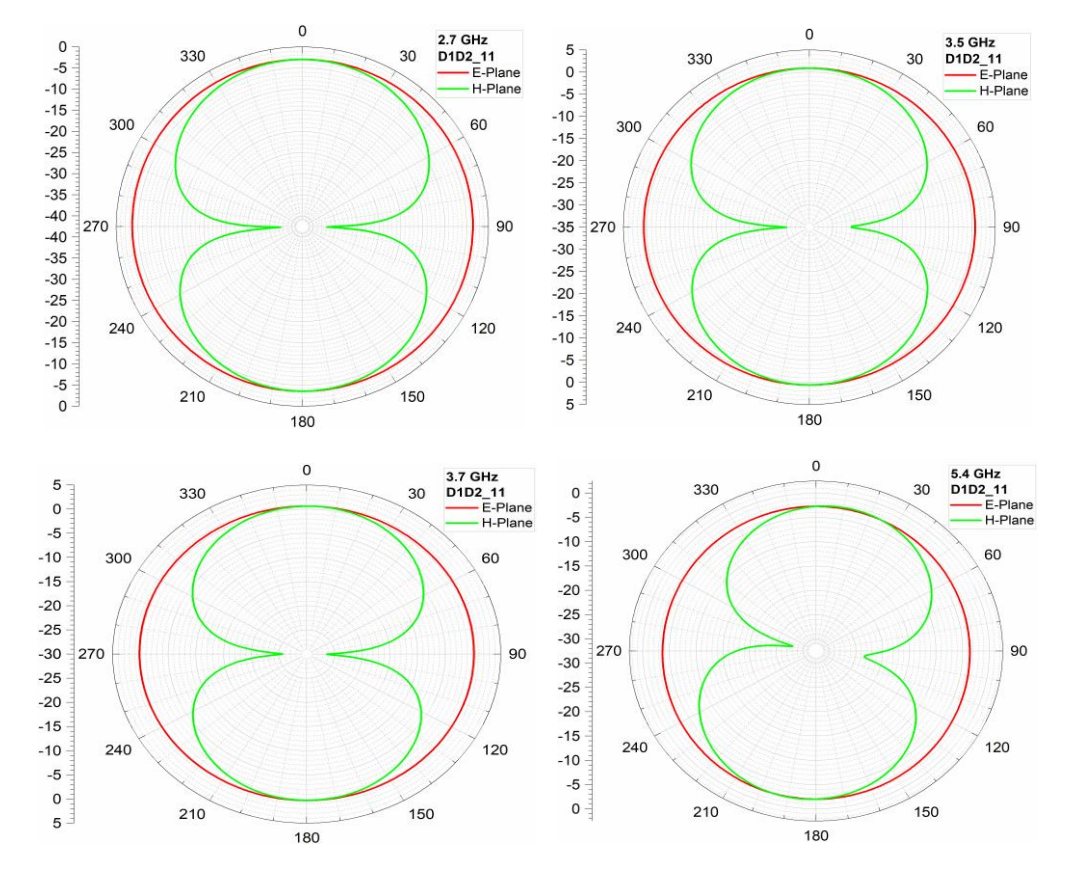


Fig 13. (D) Radiation Pattern of MMPA's at SM4, Operating Frequency Ranges are 2.7 GHz, 3.5 GHz, 3.7 GHz and 5.4 GHz.

ISSN: 2788-7669

Table 5. Shows The Gain and Efficiency of the Proposed Antenna Depends on Their Switching Mode of Operation

Switching mode Resonant frequency		Gain	Efficiency
SM1	3.6 GHZ	1.68 dB	81 %
SM2	3.7 GHz	1.07 dB	51%
SM3	3.6 GHz	1.64 dB	79%
	5.4 GHz	1.06 dB	50%
SM4	3.5 GHz	1.10 dB	55%

V. CONCLUSION

A simple MMPA (metamaterial-inspired microstrip patch antenna) is calculated and fabricated for IoT applications using frequency reconfiguration technique. The simulation performance of the designed antenna compared with the measured result with the help of KEYSIGHT FieldFox Microwave Analyzer N9917A. The Rectangular Split Ring Resonator (RSRR) with PIN diode gives four switching modes of operation. The frequency reconfiguration is achieved through the working mode of PIN diodes. The monopole antenna got reflection coefficient of $S_{11} = -30.710$ dB at center frequency of 4 GHz. The peak gain and radiation efficiency of the suggested MMPA is 1.68 dB and 81% at resonance frequency of 3.6 GHz. **Table 5** shows The Gain and Efficiency of the Proposed Antenna Depends on Their Switching Mode of Operation.

Acknowledgement

The author wishes to acknowledge and express thanks to the institutional support provided by the Microwave Lab, ECE Division, Karunya Institute of Technology and Sciences for the Antenna Fabrication and Testing.

CRediT Author Statement

The authors confirm contribution to the paper as follows:

Conceptualization: Sakthevel T C and Sugumar D; Methodology: Sakthevel T C; Software: Sugumar D; Data Curation: Sakthevel T C and Sugumar D; Writing- Original Draft Preparation: Sugumar D; Visualization: Sakthevel T C; Investigation: Sakthevel T C and Sugumar D; Supervision: Sugumar D; Validation: Sakthevel T C; Writing- Reviewing and Editing: Sakthevel T C and Sugumar D; All authors reviewed the results and approved the final version of the manuscript.

Declaration of competing interest

The authors declare that they have no known competing financial interests or personal relationships that could have appeared to influence the work reported in this paper

Data Availability Statement

The Datasets used and /or analysed during the current study available from the corresponding author on reasonable request.

Funding

No funding agency is associated with this research.

Consent to Publish

All authors gave permission to consent to publish.

Reference

- [1]. Jabire, A.H., Abana, M.A., Saminu, S., Adamu, M.J and Sadiq, A.M.5., "Equivalent Circuit of a Frequency Reconfigurable Metamaterial MIMO Antenna For Internet Of Things Applications", Nigerian Journal of Engineering Science and Technology Research, Vol. 10, No. 1, pp. 51-67, 2024
- [2]. W. A. Awan, N. Hussain, S. G. Park, and N. Kim, "Intelligent metasurface based antenna with pattern and beam reconfigurability for internet of things applications," Alexandria Engineering Journal, vol. 92, pp. 50–62, Apr. 2024, doi: 10.1016/j.aej.2024.02.034.
- [3]. J. Abraham, K. Natarajan, S. Andi, J. V. Mariyarose, M. Alagarsamy, and K. Suriyan, "Frequency reconfigurable microstrip patch antenna for multiband applications," International Journal of Reconfigurable and Embedded Systems (IJRES), vol. 13, no. 2, p. 472, Jul. 2024, doi: 10.11591/ijres.v13.i2.pp472-482.
- [4]. Z. Kudaibergenova, K. Dautov, and M. Hashmi, "Compact metamaterial-integrated wireless information and power transfer system for low-power IoT sensors," Alexandria Engineering Journal, vol. 92, pp. 176–184, Apr. 2024, doi: 10.1016/j.aej.2024.02.058.
- [5]. U. Patel et al., "Split ring resonator geometry inspired crossed flower shaped fractal antenna for satellite and 5G communication applications," Results in Engineering, vol. 22, p. 102110, Jun. 2024, doi: 10.1016/j.rineng.2024.102110.
- [6]. S. V. Pande and D. P. Patil, "Miniaturization of antenna using metamaterial loaded with CSRR for wireless applications," Bulletin of Electrical Engineering and Informatics, vol. 13, no. 2, pp. 973–985, Apr. 2024, doi: 10.11591/eei.v13i2.6362.
- [7]. J. Xue, A. Ni, L. Liu, Z. Wang, and X. Wang, "An Ultra-wideband Antenna Based on Left-handed Materials for IoT Applications," Progress In Electromagnetics Research C, vol. 140, pp. 151–161, 2024, doi: 10.2528/pierc23103103.
- [8] A. B. Shallah et al., "A Miniaturized Metamaterial-Based Dual-Band 4×4 Butler Matrix With Enhanced Frequency Ratio for Sub-6 GHz 5G Applications," IEEE Access, vol. 12, pp. 32320–32333, 2024, doi: 10.1109/access.2024.3371027.
- [9] N. K. Majji, V. N. Madhavareddy, G. Immadi, N. Ambati, and S. M. Aovuthu, "Analysis of a Compact Electrically Small Antenna with SRR for RFID Applications," Engineering, Technology & Science Research, vol. 14, no. 1, pp. 12457–12463, Feb. 2024, doi: 10.48084/etasr.6418.

- [10]. N. K. Majji, V. N. Madhavareddy, G. Immadi, and N. Ambati, "A Low-Profile Electrically Small Serrated Rectangular Patch Antenna for RFID Applications," Engineering, Technology & Engineering, Technology & Papplied Science Research, vol. 14, no. 2, pp. 13611–13616, Apr. 2024, doi: 10.48084/etasr.6989.
- [11]. C. Zhang et al., "Frequency-Self-Adaptive Radio Frequency Power Harvester Enabled by Shape-Reconfigurable Liquid Metal," Electromagnetic Science, vol. 2, no. 2, pp. 1–13, Jun. 2024, doi: 10.23919/emsci.2024.0008.
- [12]. J. Mohammed Rasool and A. Kadhum Abd, "A Reconfigurable Antenna for IoT Applications with Enhanced Performance by Adding Metamaterial," Journal of Communications, pp. 198–203, Apr. 2024, doi: 10.12720/jcm.19.4.198-203.
- [13]. T. A. Elwi et al., "On the Performance of a Photonic Reconfigurable Electromagnetic Band Gap Antenna Array for 5G Applications," IEEE Access, vol. 12, pp. 60849–60862, 2024, doi: 10.1109/access.2024.3392368.
- [14]. K. Kumar Naik and B. Venkata Sai Sailaja, "RF-MEMS Switch for Reconfigurable With Half-Moon Slots on Elliptical-Shaped Patch Antenna for 5G Applications," IEEE Open Journal of Antennas and Propagation, vol. 5, no. 3, pp. 673–685, Jun. 2024, doi: 10.1109/ojap.2024.3384397.
- [15] J. Zhang, B. Wang, S. Yan, W. Li, and G. A. E. Vandenbosch, "Metamaterial Inspired Varactor-Tuned Antenna with Frequency Reconfigurability and Pattern Diversity," Sensors, vol. 24, no. 6, p. 1956, Mar. 2024, doi: 10.3390/s24061956.
- [16]. T. Messatfa, S. Berhab, F. Chebbara, and M. S. Soliman, "Curvature-Adaptive Compact Triple-Band Metamaterial Uniplanar Compact Electromagnetic Bandgap-Based Printed Antenna for Wearable Wireless and Medical Body Area Network Applications," Processes, vol. 12, no. 7, p. 1380, Jul. 2024, doi: 10.3390/pr12071380.
- [17]. J. R. Reis, M. Vala, T. E. Oliveira, T. R. Fernandes, and R. F. S. Caldeirinha, "Metamaterial-Inspired Flat Beamsteering Antenna for 5G Base Stations at 3.6 GHz," Sensors, vol. 21, no. 23, p. 8116, Dec. 2021, doi: 10.3390/s21238116.
- [18]. A. Sabban, "Novel Meta-Fractal Wearable Sensors and Antennas for Medical, Communication, 5G, and IoT Applications," Fractal and Fractional, vol. 8, no. 2, p. 100, Feb. 2024, doi: 10.3390/fractalfract8020100.
- [19]. H. Hussein, F. Atasoy, and T. A. Elwi, "Miniaturized Antenna Array-Based Novel Metamaterial Technology for Reconfigurable MIMO Systems," Sensors, vol. 23, no. 13, p. 5871, Jun. 2023, doi: 10.3390/s23135871.
- [20]. D. N. Gençoğlan, Ş. Çolak, and M. Palandöken, "Spiral-Resonator-Based Frequency Reconfigurable Antenna Design for Sub-6 GHz Applications," Applied Sciences, vol. 13, no. 15, p. 8719, Jul. 2023, doi: 10.3390/app13158719.
- [21]. M. Hussain, W. Awan, M. Alzaidi, N. Hussain, E. Ali, and F. Falcone, "Metamaterials and Their Application in the Performance Enhancement of Reconfigurable Antennas: A Review," Micromachines, vol. 14, no. 2, p. 349, Jan. 2023, doi: 10.3390/mi14020349.
- [22]. S. A. Khaleel, E. K. I. Hamad, N. O. Parchin, and M. B. Saleh, "Programmable Beam-Steering Capabilities Based on Graphene Plasmonic THz MIMO Antenna via Reconfigurable Intelligent Surfaces (RIS) for IoT Applications," Electronics, vol. 12, no. 1, p. 164, Dec. 2022, doi: 10.3390/electronics12010164.
- [23]. H. H. Al-Khaylani, T. A. Elwi, and A. A. Ibrahim, "A Novel Miniaturized Reconfigurable Microstrip Antenna Based Printed Metamaterial Circuitries For 5g Applications," Progress In Electromagnetics Research C, vol. 120, pp. 1–10, 2022, doi: 10.2528/pierc22021503.
- [24]. S. T. Al-Hadeethi, T. A. Elwi, and A. A. Ibrahim, "A Printed Reconfigurable Monopole Antenna Based on a Novel Metamaterial Structures for 5G Applications," Micromachines, vol. 14, no. 1, p. 131, Jan. 2023, doi: 10.3390/mi14010131.
- [25]. K.Sumathi, S. Lavadiya, P. Yin, J. Parmar, and S. K. Patel, "High gain multiband and frequency reconfigurable metamaterial superstrate microstrip patch antenna for C/X/Ku-band wireless network applications," Wireless Networks, vol. 27, no. 3, pp. 2131–2146, Feb. 2021, doi: 10.1007/s11276-021-02567-5.
- [26]. S. P. Lavadiya, S. K. Patel, and R. Maria, "High gain and frequency reconfigurable copper and liquid metamaterial tooth based microstrip patch antenna," AEU International Journal of Electronics and Communications, vol. 137, p. 153799, Jul. 2021, doi: 10.1016/j.aeue.2021.153799.
- [27]. B. Ali Esmail et al., "Reconfigurable Radiation Pattern of Planar Antenna Using Metamaterial for 5G Applications," Materials, vol. 13, no. 3, p. 582, Jan. 2020, doi: 10.3390/ma13030582.
- [28]. Yaghjian, "An overview of near-field antenna measurements," in IEEE Transactions on Antennas and Propagation, vol. 34, no. 1, pp. 30-45, January 1986, doi: 10.1109/TAP.1986.1143727.

Publisher's note: The publisher remains neutral with regard to jurisdictional claims in published maps and institutional affiliations. The content is solely the responsibility of the authors and does not necessarily reflect the views of the publisher.